



Fabrication of a sugar-immobilized fluorescent PMMA shell on a Ni core particle via soap-free emulsion polymerization

Noriko Yamauchi¹ · Kensuke Yakushiji¹ · Airi Tago¹ · Ryota Saito^{2,3} · Yoichiro Sogame² · Makoto Ogata⁴ · Yoshio Kobayashi¹

Received: 6 October 2021 / Revised: 1 December 2021 / Accepted: 3 January 2022 / Published online: 14 January 2022
© The Author(s), under exclusive licence to Springer-Verlag GmbH Germany, part of Springer Nature 2022, corrected publication 2022

Abstract

Sugar chain immobilized polymer particles having both magnetic and fluorescent properties can be expected to be useful in a wide variety of biomedical applications such as the detection, separation, and purification of proteins, viruses, or bacteria, because sugar chains specifically adsorb them. Since high magnetic responsiveness is required for such applications, we attempted to fabricate core-shell particles consisting of a submicron-sized magnetic core and a thin polymer shell (nano- to dozens of nanometers thick) that incorporates a fluorescent dye, with sugar molecules immobilized on the surface. Soap-free emulsion polymerization using methyl methacrylate (MMA) monomer and potassium persulfate (KPS) initiator in the presence of aminopropyltrimethoxysilane-treated Ni particles, octyl- β -D-glucopyranoside (octyl-glc), and rhodamine B (RhB) produced a glucose-immobilized fluorescent PMMA thin shell on a Ni particle (Ni/PMMA/RhB/octyl-glc). Electrostatic interaction was used both to incorporate RhB into the PMMA shell and to coat the Ni core with the PMMA-RhB shell. Glucose was immobilized on the PMMA shell by embedding a hydrophobic octyl group derived from octyl-glc in the PMMA matrix, and the resulting sugar-immobilized PMMA shell was able to adsorb protein (concanavalin A; a protein that specifically adsorbs glucose). The resulting Ni/PMMA/RhB/octyl-glc particles were well-dispersed in water, detected by highly sensitive fluorescence techniques, and could be collected by a magnet within 10 sec. They are expected to be applied to detect biological substances such as various proteins and viruses by changing the glucose moiety of the particle surface to other functional glycans.

Keywords Colloid · Glucose · Fluorescence · Magnetic property · Polymer particle · Encapsulation

Introduction

Sugar-chain-immobilized particles can be expected to be useful in a wide variety of biomedical applications such as in the separation and purification of toxic proteins, pathogenic

viruses, or bacteria, because sugar chains are known to adsorb these toxins [1–4]. By introducing fluorescent substances into the sugar-chain-immobilized particles, highly sensitive fluorescent detection methods are made possible. In order to detect viruses quickly and accurately, one strategy is to rapidly collect particles magnetically after proteins or viruses are adsorbed on the surface [5–8]. Furthermore, particles from tens to hundreds of nanometers in size, which have a very large specific surface area and are easy to handle, are very interesting candidates to use as carriers for immobilized sugar chains [9, 10]. In addition, for suppression of oxidation and agglutination of such magnetic metal particles, it is desirable that the surface of the particles be coated with a chemically stable and non-toxic substance.

Based on the above, we thought it might be advantageous to fabricate core-shell particles consisting of a submicron-sized magnetic core and a thin polymer shell (from nano- to tens of nanometers thick) incorporating a fluorescent dye, with sugar molecules immobilized on the surface. The

✉ Noriko Yamauchi
noriko.yamauchi.12@vc.ibaraki.ac.jp

¹ Department of Materials Science and Engineering, Graduate School of Science and Engineering, Ibaraki University, 4-12-1, Naka-narusawa-cho, Hitachi, Ibaraki 316-8511, Japan

² Department of Applied Chemistry and Biochemistry, National Institute of Technology, Fukushima College, Nagao 30, Kamiarakawa, Taira, Iwaki, Fukushima 970-8034, Japan

³ Department of Chemistry and Biotechnology, Faculty of Science and Technology, Kochi University, 2-5-1 Akebono-cho, Kochi 780-8520, Japan

⁴ Faculty of Food and Agricultural Sciences, Fukushima University, 1 Kanayagawa, Fukushima 960-1296, Japan

smaller the volume ratio of the polymer shell to the magnetic core, the higher the magnetic particle content, leading to composite particles having high external magnetic field responsiveness. Therefore, a magnetic particle having a thin polymer shell can be expected to have higher magnetic properties than either small magnetic particles embedded in a polymer particle [11, 12] or small magnetic particles attached to the surface of a core particle.

Multi-step processes for fabricating multi-functional particles are expensive, require a lot of energy, are labor intensive, and are environmentally wasteful. A key characteristic of this study is that the sugar-immobilized fluorescent thin polymer shell on the magnetic core was fabricated via soap-free emulsion polymerization, which has a low environmental load and often gives impurity-free polymer particles. This is desirable because medical biotechnology applications require impurity-free, stable particles in aqueous solvent. The facile process we developed fabricates a thin polymer shell on a magnetic core, incorporates a fluorescent dye into the polymer shell, and immobilizes sugar molecules on the surface of the polymer shell, at the same time. In other words, the thin polymer shell in this study functions not only to prevent aggregation and oxidation of the magnetic particles, but also to provide a base for immobilizing both a fluorescent dye and a sugar onto the magnetic particles. Polymethyl methacrylate (PMMA), which is chemically stable and has low toxicity, was used as the polymer shell.

Electrostatic interactions were used to incorporate the fluorescent dye into the PMMA shell. Rhodamine B (RhB), which has a positive charge, was expected to have a high affinity for the PMMA shell (which is negatively charged from the initiator, potassium persulfate (KPS)). To immobilize functional sugars on the PMMA shell, we applied the unique idea we developed previously [13, 14]. Octyl- β -D-glucopyranoside (octyl-glc), glucose having a hydrophobic octyl group, was used as the functional sugar. In previous studies, we concluded that hydrophobic octyl groups implanted as anchors inside the hydrophobic submicron-sized PMMA particles tended to direct the hydrophilic glucose components to the outer aqueous phase. As a strategy to immobilize sugars having many reactive groups (e.g., OH^-), we think it is preferable to utilize methods involving hydrophobic interactions, which have no risk of sugar chain structural changes due to chemical side reactions.

Nickel was chosen as the magnetic particle because Ni has sufficient saturation magnetization, stability in the atmosphere, and low toxicity [15]. The Ni particles were prepared using the hydrazine reduction method because it allows for formation of submicron-sized Ni particles and Ni alloy particles in an aqueous solvent, and crystallization of Ni and Ni alloy without heat treatment [16–19]. Ni particles need to be crystallized in order to be externally magnetically responsive, but heat treatment of Ni particles before coating

with the polymer thin shell tends to cause aggregation of the particles. In addition, since organic substances typically have a low decomposition temperature, heat treatment of Ni particles after coating with the polymer shell is not possible. Therefore, the hydrazine reduction method, by which submicron-sized crystallized Ni particles can be fabricated without heat treatment, is ideal. In this study, in order to obtain relatively uniform-sized Ni particles (~ 200 nm), a hydrazine reduction method involving stirring with a paddle impeller as well as ultrasonic irradiation was carried out.

In order to coat an inorganic particle such as Ni with an organic polymer, it is necessary to introduce organic components to the surface of the inorganic particle to enhance affinity. Silane coupling agents have often been used to introduce organic components to the surface of an inorganic oxide particle [20–22]. Since the thin surface layer of Ni particles prepared via the aqueous hydrazine reduction method was expected to be oxidized to NiO [23], we attempted to introduce aminopropyltrimethoxysilane (APMS) onto the Ni particle surface via a dehydration condensation reaction with the hydroxy groups existing in the oxide layer on the Ni particle surface. APMS was selected not only to introduce organic components to the Ni particle surface, but also to provide a positive charge derived from the amino group to the Ni particle surface to enable electrostatic interactions with PMMA (which is negatively charged from the KPS).

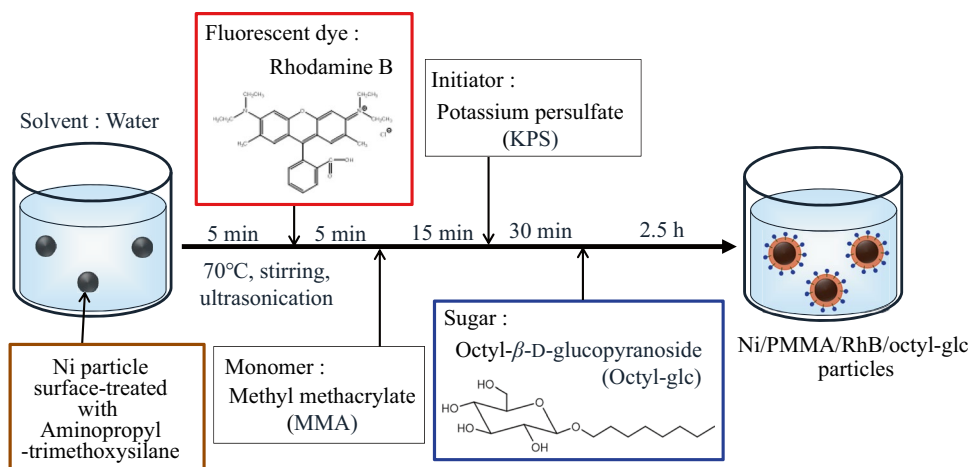
Herein, the particles obtained are evaluated for their specific adsorptivity to protein (lectin), and a fluorescence microscope is used to observe how the particles dispersed in water are rapidly attracted to a magnet.

Experimental

Materials

Ni (II) acetate tetrahydrate ($\text{Ni}(\text{CH}_3\text{COOH})_2 \cdot 4\text{H}_2\text{O}$, 97%) used as a nickel precursor, hydrazine monohydrate ($\text{N}_2\text{H}_4\text{OH}$) used as a reductant, and 1 M NaOH solution used for pH adjustment for the formation of metallic Ni nanoparticles were purchased from Kanto Chemical Co. (Japan). Poly(sodium 4-styrenesulfonate) (PSS, Mw: 70,000) used as a dispersing stabilizer, and 3-aminopropyltrimethoxysilane (APMS, 97%) used as a surface modification reagent were purchased from Sigma-Aldrich. Methylmethacrylate (MMA), used as a monomer, and potassium persulfate (KPS), used as an initiator, and rhodamine B (RhB) were purchased from Fujifilm Wako Chemicals (Japan). Octyl- β -D-glucopyranoside (octyl-glc) and concanavalin A (ConA) were purchased from Tokyo Chemical Industry Co., Ltd. (Japan) and J-CHEMICAL Inc. (Japan), respectively. The polymerization inhibitor contained in the MMA monomer was removed by using an inhibitor remover (Sigma-Aldrich).

Scheme 1 Procedure for the formation of glucose-immobilized fluorescent PMMA shells onto Ni particles (Ni/PMMA/RhB/octyl-glc)



The other reagents were used as purchased. Water was purified using an Advantec (Japan) RFD372NC water distillation apparatus.

Experimental methods

Preparation of Ni particles via the hydrazine reduction method

After adding nickel acetate (1.5 mmol), hydrazine monohydrate (1.05 mol), and 1 M NaOH solution (15 mL) to ion-exchanged water in which PSS (15 mmol) was dissolved, the mixture was stirred with a paddle impeller (250 rpm) under ultrasonication (28 kHz, 300 W) at 60 °C. The final reaction volume was 150 mL. Five minutes later, a suspension of black particles was obtained. In order to confirm the effect of ultrasonication, the experiment was conducted under the same conditions without it.

The particles obtained were washed with ion-exchanged water followed by ethanol. Then, 129 mL of ethanol was added to prepare a Ni particle suspension.

Surface-modification of the Ni particles

After stirring 129 mL of the Ni particle suspension with a paddle impeller (250 rpm) under ultrasonication (28 kHz, 300 W) at 35 °C for 5 min, 20 mL of ion-exchanged water was added to hydrolyze the APMS to be added later. After 15 min of stirring, APMS (2.41 μL) dissolved in 1 mL ethanol was added. The final reaction volume was 150 mL. The stirring and ultrasonication were continued for 1 h, to allow time for the hydrolysis/dehydration condensation reaction of APMS.

The particles obtained were washed with ethanol followed by ion-exchanged water. Then, 117 mL of ion-exchanged water was added to prepare an APMS-modified Ni particle suspension.

Fabrication of glucose-immobilized fluorescent PMMA shell onto Ni core particle (Ni/PMMA/RhB/octyl-glc) via soap-free emulsion polymerization

The procedure for the fabrication of glucose-immobilized fluorescent PMMA shells on Ni core particles is shown in Scheme 1. APMS-modified Ni particle dispersed in ion-exchanged water (39 mL) was charged in a cylindrical glass reactor with a cap through which was drilled a small hole to pass the stirring stick through, and was both stirred with a paddle impeller (400 rpm) and ultrasonicated (28 kHz, 300 W). When only ultrasonication was used without stirring, the Ni core particles were not sufficiently dispersed in the aqueous solvent. In order to form a uniform shell on the surface of the core particles, the individual core particles must be separated and dispersed in the solvent. By using both stirring with the paddle impeller and ultrasonic irradiation, it was possible to maintain the dispersed state of submicron-sized magnetic core particles that easily aggregate and settle in an aqueous solvent.

RhB (1.2 mg) was dissolved in 1 mL of ion-exchanged water, and then added to the dispersion heated to 70 °C. MMA monomer (0.53 mL, 5 mmol) was then added to the mixture. After 15 min, KPS initiator (0.108 g, 0.4 mmol) dissolved in 4 mL of ion-exchanged water was added to initiate polymerization. Thirty min later, octyl-glc (0.274 g, 0.94 mmol) dissolved in 6 mL of ion-exchanged water was added. The polymerization reaction was stirred at 70 °C for 3 h. The concentrations of MMA, KPS, and octyl-glc were 0.1 M, 8 mM, and 19 mM, respectively, based on the final volume of the aqueous phase. The final concentration of octyl-glc was 19 mM, which is lower than the critical micelle concentration of octyl-glc (20 mM). Therefore, the polymer-shell fabrication method of this study follows a soap-free emulsion polymerization mechanism.

Characterization

Microscopy

The Ni particles were observed via scanning electron microscopy (SEM) (SU5000, Hitachi). A transmission electron microscope (TEM) (JEM-2100, JEOL) and a scanning transmission electron microscope (STEM) (HD-2000, Hitachi) were used to observe the PMMA particles encapsulating the Ni particles.

An optical microscope system (Axio Scope A1, Carl Zeiss Microscopy) with a 555 nm LED laser was used to observe the Ni/PMMA/RhB/octyl-glc particles in aqueous solvent. When taking a fluorescence microscope image, the particles were suspended in 1% (w/v) methyl cellulose to suppress fine movement of the particles. A short movie was produced by dropping particles suspended in ion-exchanged distilled water near a neodymium magnet ($\phi 6$ mm).

Crystal structure and magnetic properties

The X-ray diffraction (XRD) was measured using a Rigaku Ultima IV X-ray diffractometer ($\text{CuK}\alpha$, $\lambda = 1.504\text{\AA}$). Magnetic properties were measured with a vibrating-sample magnetometer (VSM) (PPMS DYNA COOL, Quantum Design) at 25 °C. A vacuum freeze-dried powder sample was used for these measurements. The vacuum freeze drying was used instead of a simple vacuum drying to prepare these dried samples. Figure S1a, b show the photographs of Ni particles obtained after simple vacuum drying and after freeze-vacuum drying, respectively (see Supplementary Information). When the particles are dried by simple vacuum drying, the aggregation of the particles is promoted due to the water capillarity among the particles. Since the smooth and fine powder was obtained by vacuum freeze-drying, the analysis samples were prepared by vacuum freeze-drying in this study.

Dispersibility and surface charge in aqueous solvent

Dynamic light scattering (DLS) measurements and zeta potentials were acquired with a Zetasizer Nano (Malvern, $\lambda = 628$ nm).

Protein assay

In order to confirm whether or not glucose that could be selectively adsorbed by biological substances exists on the particle surface, specific adsorption was evaluated according to our previously reported method [13], which is briefly described as follows.

ConA was chosen as a protein (lectin) that specifically adsorbs glucose. A vacuum freeze-dried powder sample was used for the protein assay. The Ni particles coated with glucose-immobilized PMMA shells dispersed in ion-exchanged distilled water were mixed with 0.25 mg of ConA dissolved in 0.25 mL of 10 mM phosphate-buffered saline (PBS) at pH 7.4, and the mixture was left in an ice bath for 30 min. Next, in order to precipitate ConA adsorbed on the particle surface together with the particles, a centrifugation was performed at 18,000 G and 4 °C for 30 min. The concentration of ConA remaining in the supernatant was calculated from the absorbance (A_{280}) of the supernatant in which the residual ConA was dispersed, as measured with a Nano-100 spectrophotometer (Bio Medical Science).

Results and discussion

Preparation of Ni particle via hydrazine reduction method

First, the effect of ultrasonic irradiation on the preparation of Ni particles via hydrazine reduction was investigated. Figure 1 shows SEM images of the Ni particles prepared (a) without and (b) with ultrasonication. When only stirring with a paddle impeller without sonication (a), the particles obtained aggregated into micro-sized agglomerates. On the other hand, when ultrasonication was performed at the same time as stirring (b), smaller Ni aggregates with an average size of 200 nm were obtained. The particles obtained by stirring with ultrasonic irradiation were confirmed by XRD measurements to have a nickel crystal structure (Fig. 2a). Further structural evidence is provided by the magnetization curve of the Ni particles shown in Fig. 2b. The saturation magnetization of the Ni particles is approximately 51 emu/g, almost the same as for bulk Ni (55 emu/g) [15]. Therefore, the submicron-sized metallic Ni particles should be prepared via the hydrazine reduction method utilizing both stirring and ultrasound.

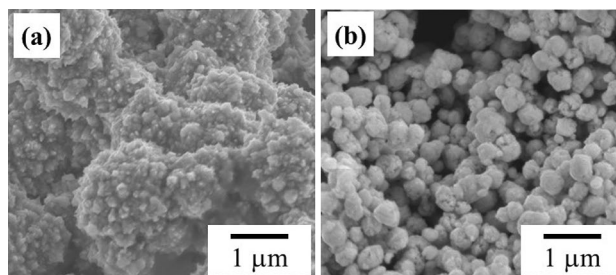
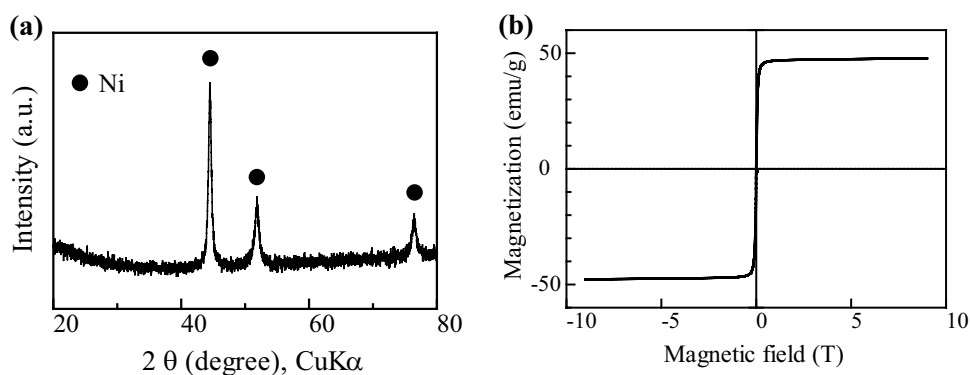


Fig. 1 SEM images of Ni particles prepared via the hydrazine reduction method with stirring (a) and with both stirring and ultrasonication (b)

Fig. 2 XRD measurement (a) and magnetization curve (b) of the Ni particles prepared with both stirring and ultrasonication



Effect of surface modification of Ni particles on PMMA coating of Ni particles

Figure 3a shows a TEM image of the particles obtained when MMA was polymerized in the presence of Ni particles without APMS. No PMMA coating could be found on the surface of these Ni particles. On the other hand, when MMA was polymerized in the presence of APMS-treated Ni particles, a PMMA coating layer was observed on the surface of the Ni particles, as shown in the TEM image in Fig. 3b. Incidentally, without the PMMA coating (Fig. 3a), the Ni particles disintegrate under ultrasonic irradiation. On the other hand, a PMMA layer appears to suppress ultrasonic destruction of the Ni particles (Fig. 3b).

Figure 4 shows zeta potentials at various pH values of APMS-treated Ni particles before and after polymerization of MMA. Compared to APMS-treated Ni particles, the zeta potential values of the particles obtained after polymerization of MMA in the presence of APMS-treated Ni particles shifted down at all pH values. This result indicates that the surface of the APMS-treated Ni particles after MMA polymerization has negative charges derived from the KPS initiator, which is further evidence that the PMMA coating layer is present on the surface of APMS-treated Ni particles.

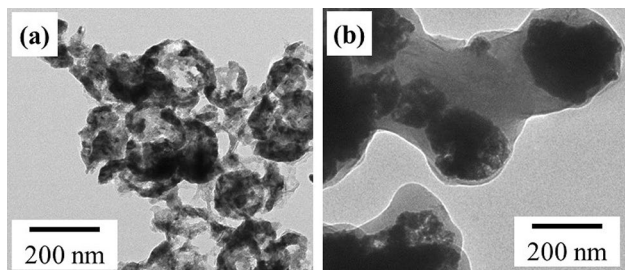


Fig. 3 TEM images of the particles obtained when MMA was polymerized in the presence of the as-prepared Ni particles (a) and Ni particles surface-treated with APMS (b)

This result also shows that metallic Ni particles synthesized in an aqueous solution can be surface-treated with APMS via a silanol reaction. This suggests that the thin surface layer of the Ni particles was oxidized and had hydroxy groups on the surface. However, from the magnetization curve in Fig. 2b, it is likely that only the thinnest layer of the Ni particle surface was oxidized and became NiO [23] when the Ni particles were formed by reduction, because the saturation magnetization value of the Ni particles is almost the same as that of bulk Ni.

Lectin adsorption ability of glucose-immobilized PMMA shells on Ni core particles

Next, PMMA shells to which octyl-glc was added were prepared 30 min after the polymerization was initiated in the presence of Ni particles, and their lectin adsorption ability was evaluated. The amount of lectin (ConA) that adsorbed on the surfaces of 3.5 mg of PMMA-shell coated Ni particles prepared with and without octyl-glc is shown in Fig. 5. The addition of octyl-glc during polymerization resulted in the formation of PMMA particles that adsorbed a larger fraction of ConA than octyl-glc-free PMMA particles. Therefore, it was found that a sufficient amount of glucose was present on the surface of the particles fabricated via this technique to specifically adsorb the protein.

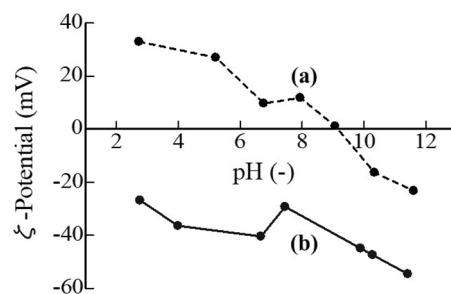


Fig. 4 Zeta potentials at various pH values of the APMS-treated Ni particles (a) and the APMS-treated Ni particles after surface-coating with PMMA (b)

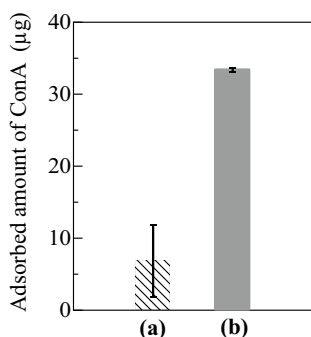


Fig. 5 Amount of lectin (ConA) adsorbed on the surface of 3.5 mg of Ni particles coated with PMMA shells fabricated without octyl-glc (a) and with octyl-glc (b)

Preparation of Ni/RhB/PMMA/octyl-glc particles

Figure 6a, b show STEM images of the particles obtained by polymerizing MMA in the presence of octyl-glc, RhB, and APMS-treated Ni particles (Ni/PMMA/RhB/octyl-glc). Figure 6a shows a secondary electron (SE) image of the particles, which have an average diameter of ca. 200 nm. The Ni particles are observed as dark regions inside the PMMA particles in the bright-field STEM (TE) image shown in Fig. 6b. The size of the Ni/PMMA/RhB/octyl-glc particles is almost the same as the size of the Ni core particles in the SEM image (Fig. 1b), suggesting the formation of a thin PMMA shell only nanometers to dozens of nanometers thick. The PMMA shell on the surface of the Ni particle was melted by

the electron beam of STEM and could not be taken clearly, so the thickness of the PMMA shell was estimated by thermogravimetric analysis (TG). The TG diagram of glucose-immobilized PMMA shells on Ni core particles is shown in Fig. S2 (see Supplementary Information). The weight ratio of Ni to PMMA in the obtained particle was estimated to be 82:18, assuming that most of the weight loss near 300 °C was due to the combustion of PMMA and Ni was hardly oxidized up to 400 °C [19]. Since the volume ratio of Ni to PMMA is 1:2, the PMMA shell can be estimated to be about 44 nm, considering that the particle size of the Ni particle is 200 nm.

When such particles are used to separate and concentrate biological substances such as proteins or viruses, a stable dispersion in water is extremely important in order to take full advantage of the large surface area of the particles. Therefore, DLS measurements were performed to evaluate the dispersibility of the particles in water. Figure 6c shows the number and volume distributions of the particles in water measured via DLS. The dispersed particle size in water is a narrow distribution; the average particle size is 300 nm, which is almost the same as the particle size obtained from the STEM image. Furthermore, this hydrodynamic size also matched the composite particle size based on the Ni core size (ca. 200 nm) in STEM observation (Fig. 6b) and the PMMA shell thickness (ca. 44 nm) estimated from the TG measurement (Fig. S2). There were almost no particles that settled during the DLS measurement. These results imply that

Fig. 6 STEM images of Ni/PMMA/RhB/octyl-glc particles (a) and (b), and number and volume distribution of Ni/PMMA/RhB/octyl-glc particles measured via DLS in water (c)

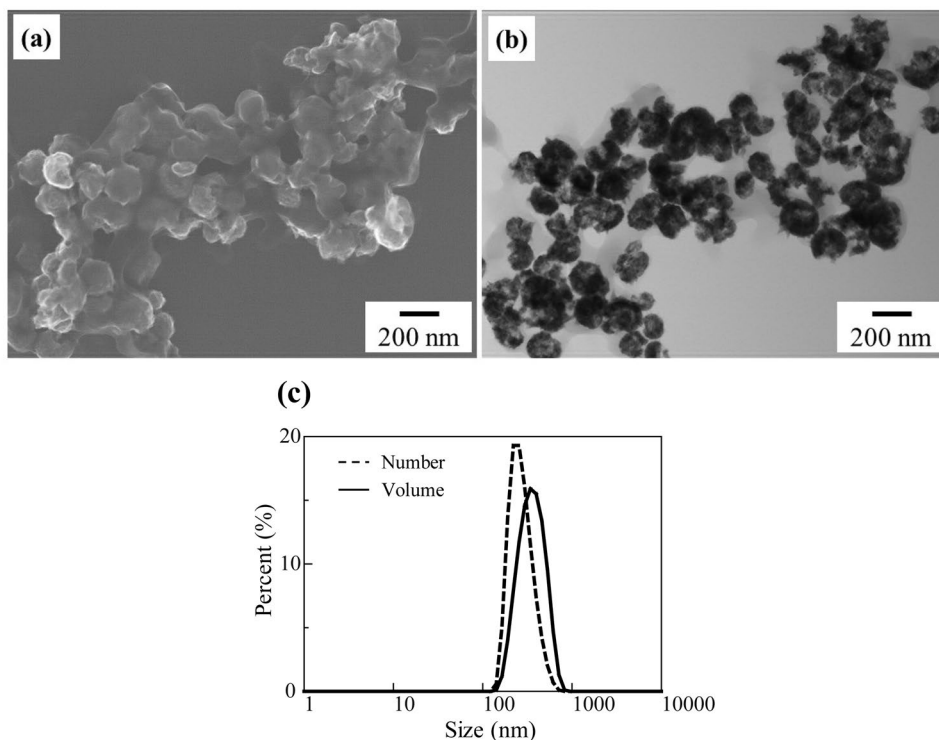
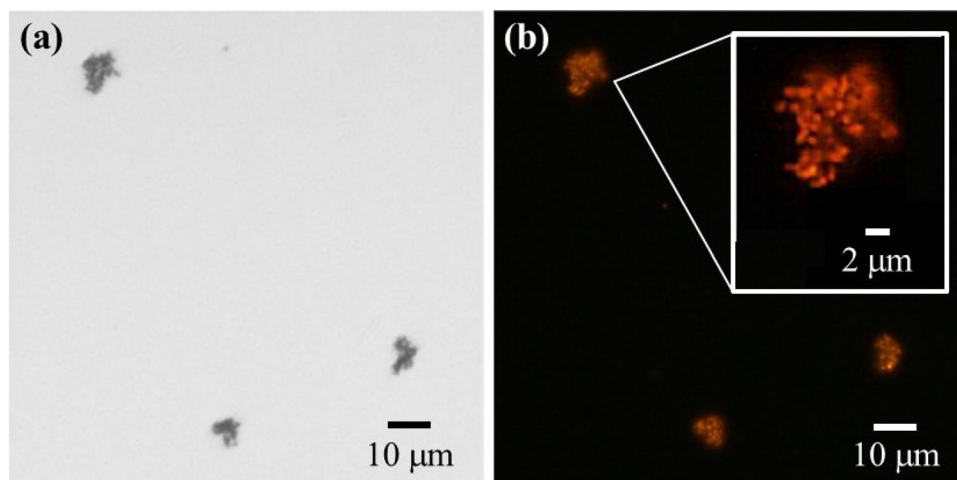


Fig. 7 Fluorescence microscope images of the aqueous-dispersed Ni/PMMA/RhB/octyl-glc particles: bright-field image (a) and fluorescence microscope image (b)



the particles are well dispersed in water during and after the formation of the glucose-immobilized PMMA shell.

The fluorescence microscope image of the aqueous-dispersed Ni/PMMA/RhB/octyl-glc particles is shown in Fig. 7. The presence of submicron-sized particles was confirmed and fluorescence was detected. Almost all of the particles observable in the bright-field image (Fig. 7a) could be observed in the fluorescence microscope image (Fig. 7b), indicating that Rhodamine B was incorporated into each particle. Since RhB is incorporated into the PMMA layer, this result suggests that a glucose-immobilized PMMA thin shell was formed on the surface of almost all of the Ni particles.

The magnetization curve of the Ni/PMMA/RhB/octyl-glc particles is shown in Fig. 8a. The Ni/PMMA/RhB/octyl-glc particles have a saturation magnetization of approximately 27 emu/g and are ferromagnetic with almost no residual magnetization. The saturation magnetization of the sample decreased from 51 emu/g of Ni particle (Fig. 2b) to 27 emu/g of the Ni/PMMA/RhB/octyl-glc particle (Fig. 8a), and the main cause of the decrease in saturation magnetization was considered to be the presence of PMMA shell and octyl-glc on the Ni particle. However, this value is as large as seven times the saturation magnetization (3.8 emu/g) of the

magnetic fluorescent polystyrene particles formed by soap-free emulsion polymerization that we previously reported [12]. Compared to the previous method of incorporating multiple 10-nm-sized magnetic particles during polymer particle formation, this method of forming a thin polymer shell on the surface of a 200-nm-sized magnetic Ni core increased the magnetic particle content of the obtained particles by more than 10 times. The increase of the magnetic particle content led to a significant improvement in external magnetic field responsiveness. The aqueous solvent in which the Ni/PMMA/RhB/octyl-glc particles dispersed was black in color (Fig. 8b). After 10 sec of placing a magnet next to the Ni/PMMA/RhB/octyl-glc particle dispersion, almost all of the particles gathered around the magnet (Fig. 8c).

In addition, we could detect the attraction of the Ni/PMMA/RhB/octyl-glc particles to a magnet with a fluorescence microscope (see Supplementary Information for the full movie of the images shown in Fig. 9). Immediately after dropping the particle suspension around the magnet, it was observed that fluorescent particles gathered around the magnet (Fig. 9b). From 2 to 10 sec, more and more particles in the aqueous solvent are attracted to the magnet (Figs. 9b–d), with no appreciable change thereafter. Therefore, the Ni/

Fig. 8 Magnetization curve of Ni/PMMA/RhB/octyl-glc particles (a) and photographs of Ni/PMMA/RhB/octyl-glc particles dispersed in water before (b) and after (c) being attracted to a magnet

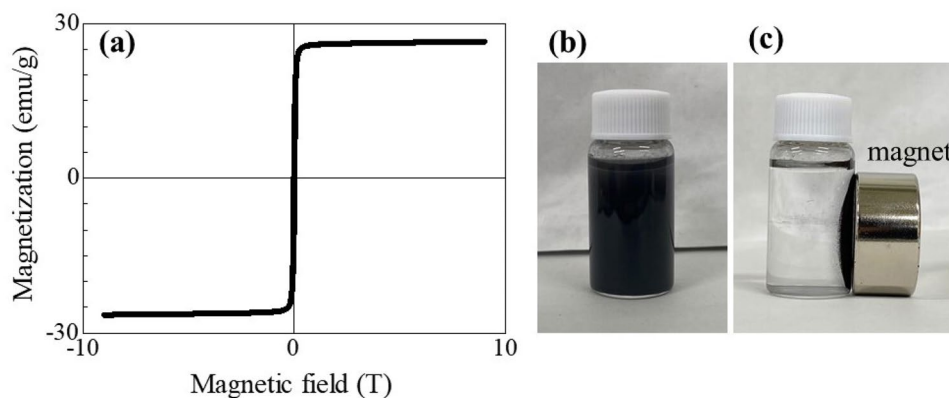
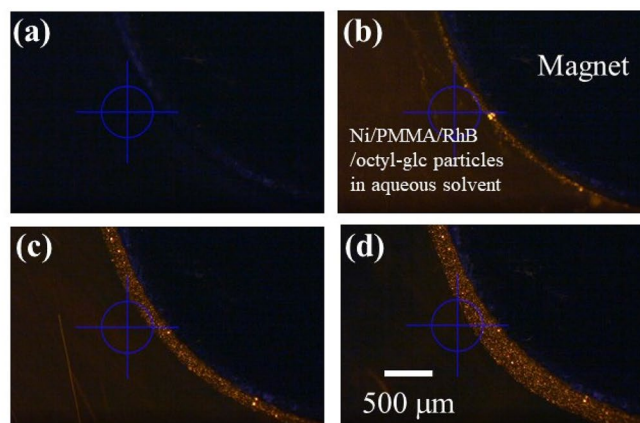
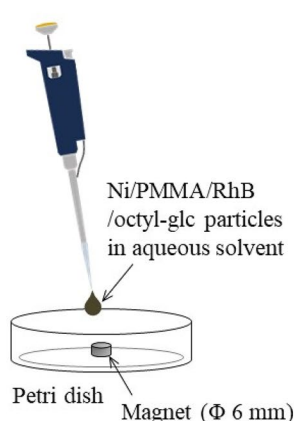


Fig. 9 Images from a short movie (Supplementary Information) of Ni/PMMA/RhB/octyl-glc particles attracted to a magnet, as observed with a fluorescence microscope. Images **a**, **b**, **c**, and **d** were captured at 0, 2, 5, and 10 sec, respectively, after dropping the colloidal suspension near the magnet on a petri dish



PMMA/RhB/octyl-glc particles prepared via this method can be rapidly magnetically separated during fluorescence detection. Going forward, by changing the glucose moiety on the particle surface to a functional glycan such as a sialo-oligosaccharide [24], these sugar-chain-immobilized particles should function as pathogenic virus (e.g., influenza virus and corona virus) detectors.

Conclusion

A thin PMMA shell incorporating RhB, with octyl-glc immobilized on the surface, was fabricated on Ni core particles via soap-free emulsion polymerization. The crystallized Ni core particles (~ 200 nm) were obtained via hydrazine reduction using both a paddle impeller and ultrasonic irradiation. APMS-derived aminopropyl groups were introduced in advance on the surface of Ni particles prepared via the hydrazine reduction method in order to increase affinity with the PMMA coating layer. The Ni particles coated with a glucose-immobilized PMMA shell were found to adsorb protein (ConA, which specifically adsorbs glucose). This result shows that our original technique of immobilizing functional sugars on the surface of a polymer particle by embedding the hydrophobic group into the polymer matrix can be applied to immobilization of functional sugars onto thin PMMA shells. When Ni/PMMA/RhB/octyl-glc particles dispersed in water were dropped near a magnet, the particles were immediately attracted to the magnet. Because the behavior of the Ni/PMMA/RhB/octyl-glc particles can be observed with a fluorescence microscope, it is suggested that after adsorbing target biological substances, the particles could be quickly collected by a magnet, and their state could be detected by fluorescence. They are expected to be applied to detect biological substances such as various proteins and viruses by changing the glucose moiety of the particle surface to other functional glycans such as a sialo-oligosaccharide.

Supplementary information The online version contains supplementary material available at <https://doi.org/10.1007/s00396-022-04945-7>.

Acknowledgements The authors are grateful to Prof Keisuke Sato (N.I.T., Ibaraki), Sanyu Co., Ltd. (Ibaraki, Japan) and Prof Munetoshi Sakai (Ibaraki U.) for supporting VSM measurements, STEM observations, and movie editing, respectively.

Funding This research was supported by JSPS KAKENHI Grant Numbers 17K18318 and 21K04764.

Declarations

Conflict of interest The authors declare no competing interests.

References

- Battigelli A, Kim JH, Dehigaspitiya DC, Proulx C, Robertson EJ, Murray DJ, Rad B, Kirshenbaum K, Zuckermann RN (2018) Glycosylated peptoid nanosheets as a multivalent scaffold for protein recognition. *ACS Nano* 12:32455–2465
- Suda Y, Zhang X, Takahashi Y, Yokoyama R, Nagatomo M, Aoyama K, Okuno T, Saito S, Morikawa S, Hiroi S, Kase T, Murakami N, Nishi J, Wakao M (2013) Discrimination of influenza virus strains and super high sensitive detection of viruses using sugar chip and sugar-chain immobilized gold nanoparticles. *Tailored Polymer Architectures for Pharmaceutical and Biomedical Applications* 20:331–350
- Ogata M, Yamanaka T, Koizumi A, Sakamoto M, Aita R, Endo H, Yachi T, Yamauchi N, Otsubo T, Ikeda K, Kato T, Park EY, Kono H, Nemoto M, Hidari KIPJ (2019) Application of novel sialoglyco particulates enhances the detection sensitivity of the equine influenza virus by real-time reverse transcriptase polymerase chain reaction. *ACS Appl Bio Mater* 2:1255–1261
- Li Y, Wang J, Sun N, Deng C (2017) Glucose-6-phosphate-functionalized magnetic microsphere as novel hydrophilic probe for specific capture of N-linked glycopeptides. *Anal Chem* 89:11151–11158
- Behra M, Azzouz N, Schmidt S, Volodkin DV, Mosca S, Chanana M, Seeberger PH, Hartmann L (2013) Magnetic porous sugar-functionalized PEG microgels for efficient isolation and removal of bacteria from solution. *Biomacromolecules* 14:1927–1935
- Zheng J, Ma C, Sun Y, Pan M, Li L, Hu X, Wuli Y (2014) Maltodextrin-modified magnetic microspheres for selective

- enrichment of maltose binding proteins. *ACS Appl Mater Interfaces* 6:3568–3574
7. Banerjee SS, Chen DH (2007) Glucose-grafted gum arabic modified magnetic nanoparticles, preparation and specific interaction with concanavalin A. *Chem Mater* 19:3667–3672
 8. Pan M, Sun Y, Zheng J, Yang W (2013) Boronic acid-functionalized core–shell-shell magnetic composite microspheres for the selective enrichment of glycoprotein. *ACS Appl Mater Interfaces* 5:8351–8358
 9. Lee JY, Cheong IW, Kim JH (2005) Agglutination study of poly (allyl- α -D-glucopyranose/styrene) latex particles in the presence of concanavalin A. *Colloids Surf B* 41:203–208
 10. Álvarez-Paino M, Juan-Rodríguez R, Cuervo-Rodríguez R, Muñoz-Bonilla A, Fernández-García M (2014) Preparation of amphiphilic glycopolymers with flexible long side chain and their use as stabilizer for emulsion polymerization. *J Colloid Interface Sci* 417:336–345
 11. Yamauchi N, Nagao D, Konno M (2010) Soap-free synthesis of highly monodisperse magnetic polymer particles with amphoteric initiator. *Colloid Polym Sci* 288:55–61
 12. Yamauchi N, Nagao D, Gu S, Konno M (2015) One pot soap-free synthesis of fluorescent, magnetic composite particles with high monodispersity. *J Chem Eng Japan* 48(7):584–587
 13. Yamauchi N, Yatabe R, Iino H, Nagatsuka M, Sogame Y, Ogata M, Kobayashi Y (2020) Spontaneous immobilization of both a fluorescent dye and a functional sugar during the fabrication of submicron-sized PMMA particles in an aqueous solution. *Colloids Surf A* 604:125299
 14. Yamauchi N, Iino H, Obinata S, Ogata M, Yatabe R, Kobayashi Y, Kurumada K (2019) One-pot formation of sugar-immobilized monodisperse polymethylmethacrylate particles by soap-free emulsion polymerization. *Colloids Surf A* 580:123754
 15. Uudeküll P, Kozlova J, Mändar H, Link J, Sihtmäe M, Käosaar S, Blinova I, Kasemets K, Kahru A, Stern R, Tätte T, Kukli K, Tamm A (2017) Atomic layer deposition of titanium oxide films on as-synthesized magnetic Ni particles: magnetic and safety properties. *J Magn Magn Mater* 429:1299–304
 16. Park JW, Chae EH, Kima SH, Lee JH, Kima JW, Yoon SM, Choi JY (2006) Preparation of fine Ni powders from nickel hydrazine complex. *Mater Chem Phys* 97:371–378
 17. Xu Z, Jin C, Xia A, Zhang J, Zhu G (2013) Structural and magnetic properties of nanocrystalline nickel-rich Fe-Ni alloy powders prepared via hydrazine reduction. *J Magn Magn Mater* 336:14–19
 18. Lu W, Sun D, Yu H (2013) Synthesis and magnetic properties of size-controlled CoNi alloy nanoparticles. *J Alloys Compd* 546(5):229–233
 19. Tago A, Yamauchi N, Nakashima K, Nagao D, Kobayashi Y (2021) Effect of silica-coating on crystal structure and magnetic properties of metallic nickel particles. *Adv Powder Technol* 32(11):4177–4185
 20. Tang E, Liu H, Sun L, Zheng E, Cheng G (2007) Fabrication of zinc oxide/poly(styrene) grafted nanocomposite latex and its dispersion. *Eur Polym J* 43:4210–4218
 21. Wang Z, Bockstaller MR, Matyjaszewski K (2021) Synthesis and applications of ZnO/polymer nanohybrids. *ACS Materials Lett* 3599–3621
 22. Okada A, Nagao D, Ueno T, Ishii H, Konno M (2013) Colloidal polarization of yolk/shell particles by reconfiguration of inner cores responsive to an external magnetic field. *Langmuir* 29(28):9004–9009
 23. Iwamoto T, Nagao A, Kitagishi K, Honjo S, Jeyadevan B (2015) Chemical synthesis of self-assembled Ni nanoparticles and understanding of nonmagnetic layer inside their surface. *J Phys Chem Solids* 87:136–146
 24. Rogers GN, D'Souza BL (1989) Receptor binding properties of human and animal H1 influenza virus isolates. *Virology* 173(1):317–322

Publisher's Note Springer Nature remains neutral with regard to jurisdictional claims in published maps and institutional affiliations.